

See discussions, stats, and author profiles for this publication at: <https://www.researchgate.net/publication/260837611>

The Actin Binding Affinity of the Utrophin Tandem Calponin-Homology Domain Is Primarily Determined by Its N-Terminal Domain

ARTICLE *in* BIOCHEMISTRY · MARCH 2014

Impact Factor: 3.02 · DOI: 10.1021/bi500149q · Source: PubMed

CITATIONS

3

READS

27

4 AUTHORS, INCLUDING:



Steve J Winder

The University of Sheffield

119 PUBLICATIONS 5,018 CITATIONS

[SEE PROFILE](#)



Krishna Mallela

University of Colorado

53 PUBLICATIONS 1,993 CITATIONS

[SEE PROFILE](#)

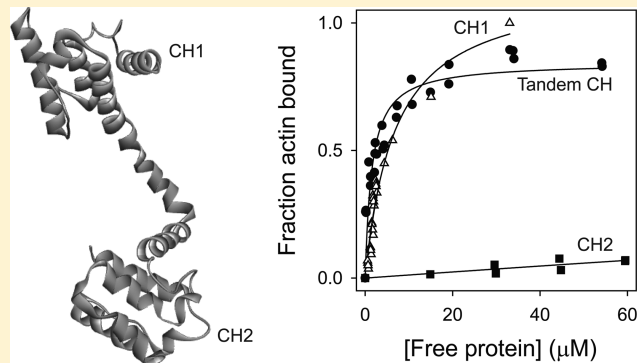
The Actin Binding Affinity of the Utrophin Tandem Calponin-Homology Domain Is Primarily Determined by Its N-Terminal Domain

Surinder M. Singh,^{†,‡} Swati Bandi,^{†,‡} Steve J. Winder,[‡] and Krishna M. G. Mallela*,[†]

[†]Department of Pharmaceutical Sciences, Skaggs School of Pharmacy and Pharmaceutical Sciences, University of Colorado Anschutz Medical Campus, Aurora, Colorado 80045, United States

[‡]Department of Biomedical Science, University of Sheffield, Western Bank, Sheffield S10 2TN, United Kingdom

ABSTRACT: The structural determinants of the actin binding function of tandem calponin-homology (CH) domains are poorly understood, particularly the role of individual domains. We determined the actin binding affinity of isolated CH domains from human utrophin and compared them with the affinity of the full-length tandem CH domain. Traditional cosedimentation assays indicate that the C-terminal CH2 domain binds to F-actin much weaker than the full-length tandem CH domain. The N-terminal CH1 domain is less stable and undergoes severe protein aggregation; therefore, traditional actin cosedimentation assays could not be used. To address this, we have developed a folding-upon-binding method. We refolded the CH1 domain from its unfolded state in the presence of F-actin. This results in a competition between actin binding and aggregation. A differential centrifugation technique was used to distinguish actin binding from aggregation. Low-speed centrifugation pelleted CH1 aggregates, but not F-actin or its bound protein. Subsequent high-speed centrifugation resulted in the cosedimentation of bound CH1 along with F-actin. The CH1 domain binds to F-actin with an affinity similar to that of the full-length tandem CH domain, unlike the CH2 domain. The actin binding cooperativity between the two domains was quantitatively calculated from the association constants of the full-length tandem CH domain and its CH domains, and found to be much smaller than the association constant of the CH1 domain alone. These results indicate that the actin binding affinity of the utrophin tandem CH domain is primarily determined by its CH1 domain, when compared to that of its CH2 domain or the cooperativity between the two CH domains.



Tandem calponin-homology (CH) domains form a major class of actin-binding domains in proteins.^{1,2} Despite their importance, the functional role of individual structural elements is not well understood. This molecular knowledge could be used to develop effective therapies for associated muscle diseases,¹ such as Duchenne/Becker muscular dystrophy (DMD/BMD). Genetic mutations in dystrophin trigger DMD/BMD because of the decrease in the net concentration of functional dystrophin.^{3–5} Dystrophin stabilizes the muscle cell membrane against the mechanical forces associated with muscle contraction and stretch by connecting actin filaments to the sarcolemmal glycoprotein complex.^{3,6} Utrophin is the closest homologue of dystrophin and functions like dystrophin. It has been proposed as a potential protein drug to treat dystrophin loss in DMD/BMD patients.^{7–9} Therefore, understanding the structure–function relationship of utrophin could lead to more effective DMD/BMD therapies. Both dystrophin and utrophin contain two calponin-homology (CH) domains in tandem at their N-termini, with which they bind to F-actin. In this study, we focus specifically on the role of the individual CH domains in the actin binding of the utrophin tandem CH domain.

Previous actin binding experiments with tandem CH domains used truncated protein constructs,¹⁰ but they did not provide a clear understanding of the specific protein regions that control function. Actin binding of a few truncated proteins was successfully monitored; however, experiments on a majority of truncated proteins were unsuccessful. The major problems were obtaining high yields of pure proteins and the decreased solubility of the truncated proteins. To enhance the solubility, proteins were fused with maltose-binding protein (MBP),^{11–13} which is much larger (387 amino acids) than the truncated protein constructs. Therefore, the results obtained from these fusion proteins are ambiguous, because MBP may force the truncated constructs to adopt non-native folds, affecting actin binding. Parallel experiments examining actin binding using small, synthetic peptides indicated three possible actin-binding surfaces (ABSs).^{14,15} However, subsequently determined crystal structures of full-length tandem CH domains indicate that these three ABSs are oriented in opposite directions,^{16,17} leading to the question of whether all three

Received: February 3, 2014

Published: March 5, 2014

ABSSs are equally important for actin binding. Comparison of the sequences of the three ABSSs from peptide binding experiments with that of the utrophin indicates that its N-terminal CH domain (CH1) contains ABS1 and ABS2, whereas the C-terminal CH domain (CH2) contains ABS3¹⁸ (Figure 1).

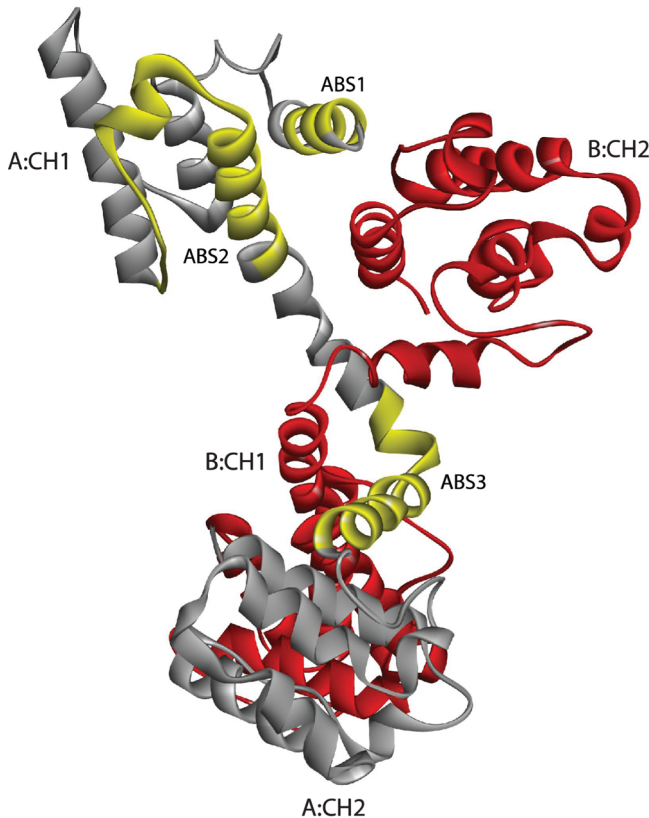


Figure 1. X-ray crystal structure of the tandem CH domain of human utrophin (Protein Data Bank entry 1QAG). Although this domain has been shown to be a monomer in solution,^{16,35} it crystallizes as an antiparallel, domain-swapped dimer.¹⁶ The two monomers, labeled A and B, are colored gray and red, respectively. The three actin-binding surfaces (ABSSs) identified from earlier peptide binding experiments^{14,15} are colored yellow in monomer A.

Experiments with truncated utrophin constructs indicate that the part of CH1 containing ABS1 binds to F-actin¹⁸ without ABS2 or ABS3, but its actin binding affinity was not measured. Consistently, an ABS1-targeting monoclonal antibody has been shown to inhibit actin binding.¹⁹ Another truncated construct containing part of ABS2 in the CH1 and CH2 domain binds to F-actin, but with decreased affinity compared to that of the full-length tandem CH domain,¹⁸ indicating that ABS1 is needed for efficient binding. Experiments with other truncated utrophin constructs, in particular the isolated CH1 domain, were less successful, because of the decreased protein stability and increased extent of aggregation.

We have developed a novel folding-upon-binding technique to measure the actin binding of the unstable CH1 domain, where we refolded the protein in the presence of F-actin. Our results show that CH1 binds F-actin with an affinity similar to that of the full-length tandem CH domain, when compared with that of the isolated CH2 domain.

MATERIALS AND METHODS

Cloning, Expression, and Purification of the Utrophin Tandem CH Domain and Its Isolated CH Domains.

Expression plasmids for the full-length tandem CH domain of utrophin (residues 1–261) were cloned from the corresponding cDNA into two different vectors, pET28a (Invitrogen) and pET-SUMO (a kind gift from C. Lima, Sloan-Kettering Institute, New York, NY). The restriction sites used were NdeI and HindIII for pET28a, and BamHI and XhoI for pET-SUMO. Plasmids were amplified using a Qiagen miniprep kit, and the constructs were confirmed by DNA sequencing. The expression plasmid for the isolated CH1 domain (residues 1–146) was created by introducing a stop codon using the quick mutagenesis protocol (Qiagen). The expression plasmid for the isolated CH2 domain (residues 147–261) was generated by subcloning the corresponding cDNA into pET-SUMO. Proteins were expressed in *Escherichia coli* BL21(DE3) cells and purified using nickel affinity chromatography. Both the full-length tandem CH domain and its isolated CH2 domain were expressed in the soluble fraction. For these two proteins expressed using pET-SUMO plasmids, the N-terminal SUMO tags were cleaved using UlpI protease. The isolated CH1 domain was expressed in inclusion bodies in both pET28a and pET-SUMO expression plasmids. The inclusion bodies were solubilized in 8 M urea; however, the protein could not be refolded by diluting the denaturant, and most of the protein aggregated. Instead, CH1 was purified in the presence of 8 M urea using Ni affinity chromatography. Pure CH1 in 8 M urea was dialyzed against PBS buffer [0.1 M NaH₂PO₄ and 0.15 M NaCl (pH 7)] to remove the imidazole present in eluted fractions from the Ni affinity column. The aggregated protein was resolubilized in PBS buffer containing 8 M urea, and this denatured pure CH1 was used for actin binding experiments.

Refolding Yield. Refolding of the tandem CH domain and its isolated CH domains was initiated by diluting 10 μM protein in 8 M urea 10-fold in PBS buffer. The samples were centrifuged at 30000g to pellet protein aggregates, and the protein concentration in the supernatants was quantified using the absorbance at 280 nm. Molar extinction coefficients for the three proteins were calculated from their amino acid sequences using PROTPARAM (<http://expasy.ch>). The protein concentration in the supernatant was used to determine the percent refolding yields.

Circular Dichroism (CD). The CD of 1 μM proteins in PBS buffer was measured using a Chirascan Plus spectrometer (Applied Photophysics). The mean residue ellipticity (MRE) was calculated from the measured CD values in millidegrees using the formula

$$\text{MRE} = (\text{CD in millidegrees}) \\ /(\text{path length in millimeters} \times \text{the molar concentration} \\ \text{of protein} \times \text{the number of residues}) \quad (1)$$

Thermal Melts. For 1 μM full-length tandem CH domain in PBS buffer, changes in the far-UV CD signal at 222 nm (ChirascanPlus spectrometer, Applied Photophysics) were monitored as a function of increasing temperature at a rate of 1 °C/min. The data were fit to a two-state unfolding model using SigmaPlot to determine the midpoint temperature (T_m) values.

Traditional Cosedimentation Assays for Measuring Actin Binding of the Full-Length Tandem CH Domain

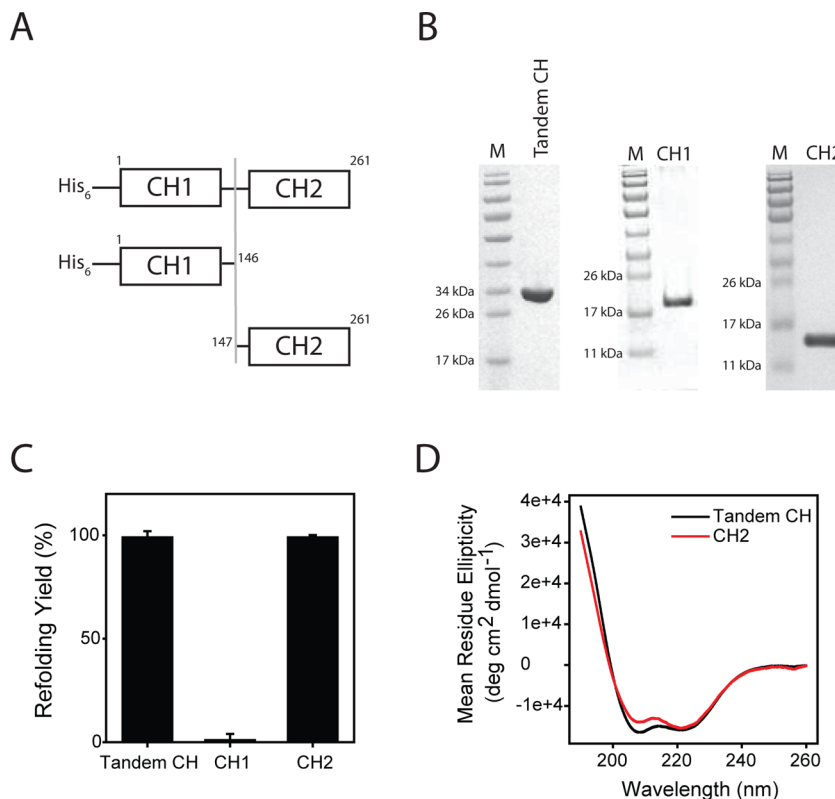


Figure 2. (A) Protein constructs used in this study: tandem CH domain (residues 1–261), CH1 (residues 1–146), and CH2 (residues 147–261). The isolated CH1 domain could not be expressed as a soluble protein, and hence, the tags could not be cleaved with proteases. The study was performed with a His-tagged tandem CH domain and a His-tagged CH1 domain. Because the CH2 domain was expressed as a soluble protein, tag-free CH2 was used. As a result, the isolated CH domains used in this study were identical to the domains in the full-length tandem CH domain with a His tag. We further confirmed that the presence of a His tag did not affect the protein function (Figure 3B), protein structure (Figure 3C), or protein stability (Figure 3D). (B) SDS-PAGE of the purified full-length tandem CH domain and its isolated CH domains. Lanes labeled M contained the molecular weight markers. (C) Refolding yields of the three proteins. (D) Circular dichroism (CD) spectra of the full-length tandem CH domain (black) and CH2 (red). Consistent with the X-ray crystal structures of the tandem CH domain (Figure 1) and the isolated CH2 domain (Protein Data Bank entry 1BHD), both proteins are α -helical.

and Its Isolated CH2 Domain. We have used the standard actin cosedimentation assays that have been developed previously.^{20,21} Skeletal muscle G-actin (43 kDa; cytoskeleton) was polymerized (final concentration of 7 μ M) to F-actin and incubated with varying concentrations of the tandem CH domain or CH2 domain at room temperature; 100 μ L was centrifuged at 100000g for 30 min (sw55Ti rotor, Beckman Optima LE80K), and the pellets were solubilized in 30 μ L of sodium dodecyl sulfate–polyacrylamide gel electrophoresis (SDS–PAGE) loading buffer. The sample was boiled, subjected to SDS–PAGE, and stained with Coomassie blue. The band intensities were determined using Quantity One on the Bio-Rad Gel Doc XR instrument, and these intensities were multiplied with the correction factors obtained from the BSA reference curve (see below) to account for differential staining of proteins with Coomassie blue.²² The ratio of the corrected intensities was used to determine the fraction of bound F-actin using the formula

$$\text{fraction actin bound} = (\text{corrected band intensity of the bound protein} \times \text{molecular weight of actin}) / (\text{corrected band intensity of actin} \times \text{molecular weight of the bound protein}) \quad (2)$$

The free protein concentration was calculated using the formula

$$\text{free protein} = \text{total protein added} - (\text{fraction actin bound} \times \text{concentration of actin added}) \quad (3)$$

Folding-upon-Binding and Differential Centrifugation Assays for Measuring Actin Binding of the Isolated CH1 Domain. A protocol similar to that described above for the traditional actin binding cosedimentation assays was followed, with the exception that the binding reaction was initiated starting from denatured CH1 in 8 M urea and the denaturant was diluted 20-fold in the presence of F-actin (final protein concentration of 7 μ M after dilution). This results in a competition between folding upon binding and protein aggregation. Aggregates were removed using low-speed centrifugation (10000g for 10 min). Supernatants from low-speed centrifugation were subjected to high-speed centrifugation (100000g for 30 min). The pellet was loaded onto an SDS–PAGE gel. Corrected band intensities were used to determine the fraction of actin bound (eqs 2 and 3). In these experiments, multiple stock concentrations of CH1 in 8 M urea were used to ensure that 5 μ L of CH1 was added to a final volume of 100 μ L, resulting in varying concentrations of CH1 while maintaining a constant urea concentration.

Determining the Correction Factors for the Differential Staining of Coomassie Blue to Actin and CH Domains. Varying bovine serum albumin (BSA) concen-

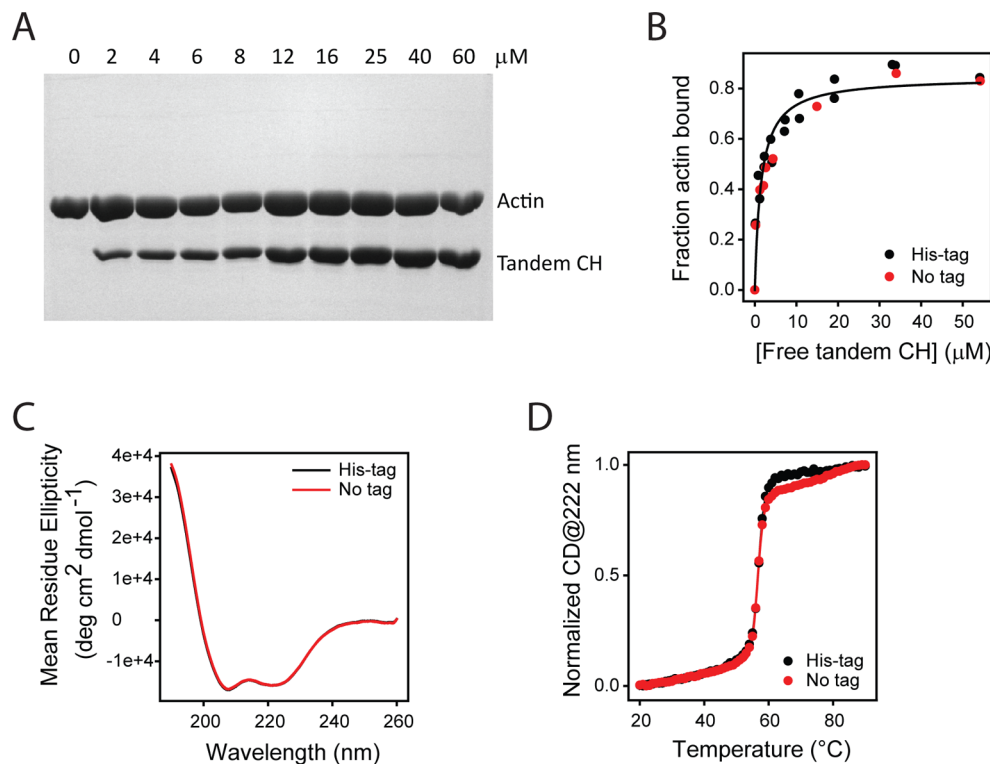


Figure 3. Actin binding cosedimentation assays of the full-length tandem CH domain. (A) SDS-PAGE of the pellets from high-speed centrifugation (100000g for 30 min) performed at a fixed concentration of F-actin (7 μM) and with varying concentrations of the tandem CH domain (0–60 μM). (B) Fraction of actin bound as a function of free protein concentration. Values were calculated from densitometry of SDS-PAGE (panel A) and corrected for differential staining of the proteins by the dye.²² The solid line indicates the global fit to the binding data obtained from three independent sets of experiments. Table 1 lists the obtained fit parameters. The presence of a His tag has no effect on actin binding, which is evident from the binding data of His-tagged (black circles) and untagged (red circles) proteins. The CD spectra (panel C) and thermal melting (panel D) of His-tagged (black) and untagged (red) tandem CH domains were identical, indicating that the presence of a His tag did not affect protein structure or stability.

trations (as determined using the micro-BCA assay from Pierce) were loaded onto SDS-PAGE gels, and the band intensities were quantified as described above. These values were used to generate a reference curve of band intensity versus protein concentration. Similar curves were generated for actin and the CH domains and were compared with that of BSA to calculate the correction factors to obtain true protein concentrations. The correction factors were 1.5 for actin and 1 for the tandem CH domain and for its isolated CH domains.

Determining K_d Values from the Actin Binding Curves. The binding curves were obtained by plotting the fraction actin bound (eq 2) versus the free protein concentration (eq 3) and were fit to the equation

$$\text{fraction actin bound} = (B_{\max}x)/(K_d + x) \quad (4)$$

where x is the free protein concentration, B_{\max} is the maximal number of binding sites, and K_d is the dissociation constant.

RESULTS

The N-Terminal CH1 Domain Is Unstable and Has a Higher Aggregation Propensity Than the C-Terminal CH2 Domain and the Full-Length Tandem CH Domain.

We initially cloned the full-length utrophin tandem CH domain (residues 1–261) and individual CH domains (CH1, residues 1–146; CH2, residues 147–261) in a pET-SUMO expression vector, where the His-SUMO tag can be cleaved using Ulp1 protease.²³ When expressed in *E. coli*, the CH1 domain was expressed in inclusion bodies, whereas both the CH2 domain

and the full-length tandem CH domain were expressed as soluble proteins. The CH1 was purified in its denatured form by solubilizing the inclusion bodies in a high denaturant concentration (8 M urea). However, CH1 could not be refolded by diluting the denaturant, and most of the protein precipitated as aggregates. Hence, the SUMO tag could not be cleaved from the CH1 construct, because the protease is not active in its denatured state. We recloned the CH1 with a His tag. A His tag is much smaller than the MBP tag used in previous studies.^{11–13} A His tag is the most commonly used tag in protein structure studies²⁴ and has been shown to have little effect on protein structure and function.^{24,25} To generate the identical full-length tandem CH domain for protein structure–function comparison, we also cloned the full-length protein with a His tag. Because CH2 was expressed as a soluble protein, the SUMO tag could be cleaved with the Ulp1 protease, and hence, CH2 without any tag was used in these studies. The final constructs are shown in Figure 2A.

Figure 2B shows SDS-PAGE of the three proteins purified to single-band homogeneity. As stated above, His-tagged CH1 could not be refolded from its denatured state, as most of the protein formed aggregates. To confirm the aggregation propensities and to show the reversibility of folding, we denatured the three proteins using 8 M urea and refolded them by diluting the denaturant 10-fold. The refolding yield was 100% for both CH2 and the full-length tandem CH domain, whereas it was ~0% for the CH1 domain (Figure 2C). The full-length tandem CH domain and CH2 refolded to their native

states as measured by their characteristic CD spectra. Both the tandem CH domain and CH2 are α -helical in solution (Figure 2D), which is consistent with the X-ray crystal structures of the tandem CH domain (Protein Data Bank entry 1QAG) and the isolated CH2 domain²⁶ (Protein Data Bank entry 1BHD). These results indicate that CH1 is unstable and has a tendency to aggregate compared with the full-length tandem CH domain and isolated CH2.

Actin Binding Affinity of the Full-Length Tandem CH Domain. Traditional actin cosedimentation assays, which have been in use in the literature for more than three decades,^{20,21} were used to measure the actin binding affinity of the utrophin tandem CH domain. Briefly, varying concentrations of the protein (0–60 μ M) were added to a solution containing a fixed concentration of F-actin (final concentration of 7 μ M) and were centrifuged at high speed (100000g for 30 min) to separate the free protein from the protein bound to F-actin. The unbound tandem CH protein remains in the supernatant, whereas F-actin and the tandem CH domain bound to the F-actin pellet. The concentration of the bound protein was determined using SDS-PAGE (Figure 3A). The band intensities were quantitated using densitometry and were corrected using bovine serum albumin (BSA) as a standard to account for the differences in the binding of Coomassie blue to different proteins.²² These corrected values were used to calculate the fraction of actin bound as a function of the free tandem CH domain concentration (Figure 3B).

The actin binding experiment described above was performed on the His-tagged tandem CH domain, so that its binding can be compared with that of the isolated CH1 domain that has the His tag. To exclude the possibility of the His tag influencing actin binding, we also performed cosedimentation assays on the untagged tandem CH domain obtained after cleaving the His-SUMO tag from the protein expressed using the pET-SUMO vector. Figure 3B compares the actin binding of the tandem CH domain with no tag (red symbols) with that of the His-tagged protein (black symbols). The binding was identical, indicating that the presence of the His tag had no effect on actin binding. We further show that the His tag did not affect the protein structure as determined by identical CD spectra (Figure 3C). The presence of a His tag also did not affect protein stability, as both untagged and tagged proteins melt with identical midpoint temperatures (T_m) in thermal melts (Figure 3D).

Fitting of the three independent data sets, two on the tagged protein and one on the untagged protein, in the binding curve (Figure 3B) globally to a standard binding equation (eq 4) resulted in a $K_{d,\text{tandem CH}}$ of $1.51 \pm 0.28 \mu\text{M}$ and a B_{\max} of 0.85 ± 0.03 (Table 1). The B_{\max} value of ~ 1 indicates that the utrophin tandem CH domain binds actin with a 1:1 stoichiometry, consistent with earlier cryo-EM studies.^{27–29}

The CH2 Domain Binds to F-Actin with a Much Decreased Affinity Compared to That of the Full-Length

Table 1. K_d and B_{\max} Values Obtained by Fitting the Binding Curves of the Utrophin Tandem CH Domain (Figure 3B) and Its Isolated CH Domains (Figures 4B and 5B)

protein	K_d (μM)	B_{\max}
tandem CH domain	1.51 ± 0.28	0.85 ± 0.03
CH1	6.81 ± 0.89	1.15 ± 0.08
CH2	>1000	1 (fixed)

Tandem CH Domain. Similar to the full-length tandem CH domain, traditional actin cosedimentation assays^{20,21} were used to measure actin binding of the CH2 domain. The CH2 used in this study was not tagged. Figure 4A shows SDS-PAGE of the

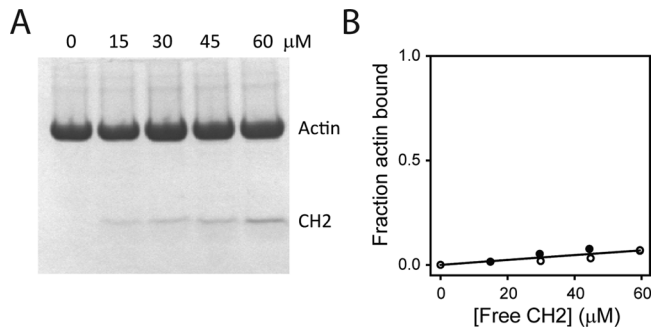


Figure 4. Actin binding cosedimentation assays of the CH2 domain. (A) SDS-PAGE of the pellets from high-speed centrifugation (100000g for 30 min) performed at a fixed concentration of F-actin (7 μM) and varying concentrations of CH2 (0–60 μM). (B) Fraction of actin bound as a function of free CH2 concentration, calculated from the band intensities from SDS-PAGE (panel A) and after correction for the differential staining of proteins with Coomassie blue.²² The solid line indicates the global fit to the binding data obtained from two independent sets of experiments. Table 1 lists the obtained fit parameters.

pellets resulting from high-speed centrifugation (100000g for 30 min) of F-actin (7 μM) with varying concentrations of CH2 (0–60 μM). Figure 4B shows the actin binding curve calculated from the densities of corresponding protein bands on SDS-PAGE corrected for the differential staining of the dye using BSA as the reference.²² The binding did not reach saturation even at the highest CH2 concentration used (60 μM). Hence, we could estimate only the lower limit for its K_d . The CH2 domain binds to F-actin with a $K_{d,\text{CH2}}$ of $>1000 \mu\text{M}$ (Table 1). For this data fitting, B_{\max} was fixed to 1. When compared with the actin binding of the full-length tandem CH domain (Figure 3B and Table 1), the CH2 domain binds to F-actin with a much decreased affinity.

Folding-upon-Binding and Differential Centrifugation Techniques for Measuring the Actin Binding Affinity of Unstable CH1. Since CH1 was purified in its denatured state and could not be refolded, traditional actin cosedimentation assays could not be used, because these assays require stable, soluble proteins. Instead, we developed a folding-upon-binding strategy. We refolded the CH1 from its denatured state in 8 M urea by diluting the denaturant 20-fold in the presence of F-actin. This results in a competition between actin binding and protein aggregation. To separate these two processes, we used a differential centrifugation technique. Low-speed centrifugation pelleted the protein aggregates, but not F-actin or its bound protein. The supernatant was subjected to high-speed centrifugation, which resulted in the cosedimentation of F-actin and CH1 bound to F-actin. The speed and the times for the two centrifugation steps had to be optimized. Multiple controls involving just CH1 without F-actin and also F-actin without CH1 were run under identical experimental conditions.

Figure 5A shows SDS-PAGE at different stages during the folding-upon-binding reaction at 5 μM CH1. Lanes 1–3 show the pellet from the low-speed centrifugation of the sample (actin with CH1) and the two controls (CH1 only and F-actin only), respectively. Lanes 4–6 show the pellets from

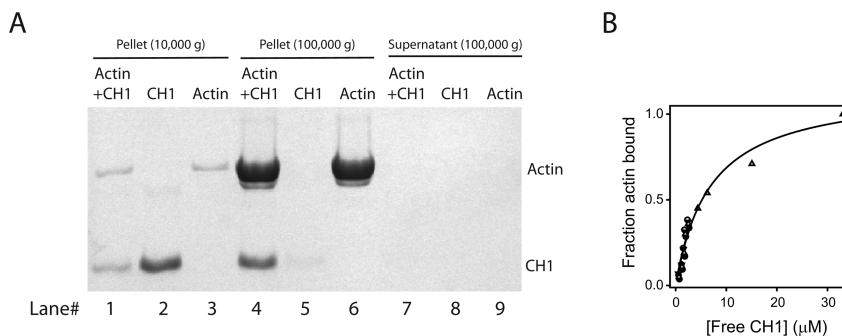


Figure 5. Folding upon binding and differential centrifugation to measure the actin binding of CH1. Denatured CH1 in 8 M urea was refolded by diluting the denaturant 20-fold in the presence of 7 μ M F-actin. As a control, unfolded CH1 was refolded in the absence of F-actin. F-Actin alone in 0.4 M urea without CH1 was used as a second control. The three samples were initially subjected to low-speed centrifugation to pellet the aggregates but not F-actin or CH1 bound to F-actin. The supernatants were then subjected to high-speed centrifugation, and SDS-PAGE of the pellets was used to quantify the fraction of actin bound. Panel A shows the result at one CH1 concentration (final concentration of 5 μ M). The figure shows SDS-PAGE of the pellets when the three samples were subjected to low-speed centrifugation (10000g for 10 min, lanes 1–3), the pellets when the supernatants of low-speed centrifugation were subjected to high-speed centrifugation (100000g for 30 min, lanes 4–6), and the supernatants after high-speed centrifugation (lanes 7–9). Lanes 2 and 5 show that all the CH1 aggregates were pelleted during the low-speed centrifugation step. Lane 9 shows that the residual urea (0.4 M) did not depolymerize F-actin. (B) Fraction of actin bound as a function of free CH1 concentration, calculated from the corrected band intensities of multiple SDS-PAGE gels. The solid line indicates the global fit to the binding data obtained from four independent sets of experiments. Table 1 lists the obtained fit parameters.

subsequent high-speed centrifugation of the supernatants. Lanes 7–9 show the supernatants following high-speed centrifugation. Low-speed centrifugation (10000g for 10 min) did not significantly pellet F-actin (lane 3) or the actin–CH1 complex (lane 1), when compared with the CH1 aggregates pelleted (lane 2). Centrifugation of the low-speed supernatants at high speed (100000g for 30 min) shows no CH1 aggregates either in the high-speed pellet (lane 5) or in the supernatant (lane 8), indicating that all the CH1 aggregates are pelleted during the low-speed centrifugation step. Therefore, the protein bands seen in the high-speed centrifugation pellet of the sample of actin and CH1 (lane 4) correspond to just actin and actin-bound CH1. The actin control (lane 6) shows that the high-speed centrifugation parameters used were sufficient to pellet all of the F-actin. SDS-PAGE of the supernatants following high-speed centrifugation (lanes 7–9) did not show any proteins, indicating that all the CH1 protein aggregated in the absence of F-actin, and the residual urea (0.4 M) present in the buffer following 20-fold dilution of the denaturant did not cause F-actin depolymerization.

The relative concentrations of F-actin and actin-bound CH1 in the pellets following high-speed centrifugation were determined from the band intensities on SDS-PAGE corrected for the differential staining of the dye. Although the low-speed centrifugation step pelleted all the CH1 aggregates at low CH1 concentrations, we did observe protein aggregation during both low- and high-speed centrifugation at CH1 concentrations of $>20 \mu$ M, irrespective of the speed and time we used for the low-speed centrifugation. In those cases, we subtracted the control (CH1 only) from the sample (actin and CH1) to obtain the fraction of actin bound. Figure 5B shows the actin binding curve of CH1. Data fitting of four independent sample sets to the binding equation (eq 4) resulted in a $K_{d,CH1}$ of $6.81 \pm 0.89 \mu$ M and a B_{max} of 1.15 ± 0.08 (Table 1). The B_{max} value of ~ 1 implies that CH1 binds to actin with a 1:1 stoichiometry.

The Actin Binding Affinity of the Tandem CH Domain Originates Primarily from the CH1 Domain. When the actin binding curves of the isolated CH domains are compared with those of the full-length tandem CH domain (Figure 6), the amount of CH1 bound to F-actin is much higher than that of the CH2 domain and is close to the values for the tandem CH domain.

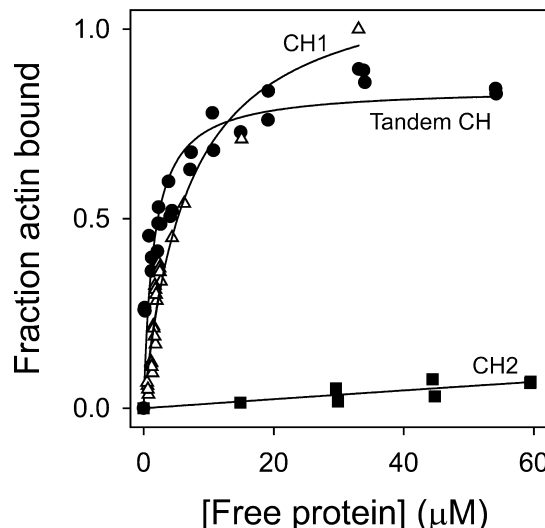


Figure 6. Comparison of actin binding of the full-length tandem CH domain (●) and its isolated CH1 (Δ) and CH2 (■) domains. CH1 binds to F-actin with an affinity similar to that of the full-length tandem CH domain. In comparison, isolated CH2 binds very weakly to F-actin.

amount of CH2 and is close to the amount of the full-length tandem CH domain at all protein concentrations. The K_d values obtained from data fitting are determined by the protein concentrations in the rising edge of the binding curve. Figure 7 shows a more detailed view of the fraction of actin bound at these low protein concentrations. The amount of CH1 bound to F-actin is much higher than that of the CH2 domain and is close to the values for the tandem CH domain.

Cooperativity between the Two CH Domains in the Actin Binding of the Full-Length Tandem CH Domain. The fact that the K_d of the tandem CH domain is slightly higher than that of the CH1 domain (Figure 6) indicates that the functional cooperativity in terms of actin binding does exist between the two CH domains. When there is no cooperativity, the association constant of the tandem CH domain, $K_{a,tandem\ CH}$, will be the sum of the association constants of the two

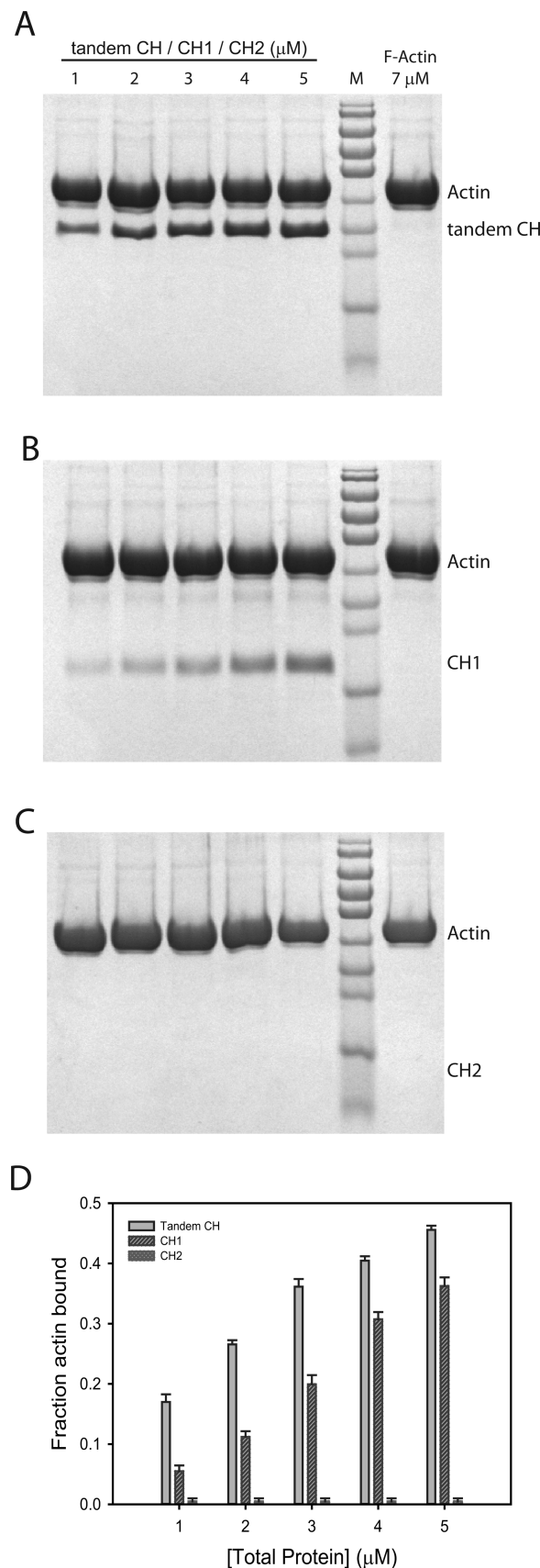


Figure 7. Comparison of actin binding of the full-length tandem CH domain and its isolated CH domains at five protein concentrations in the rising edge of the binding curve (Figure 6). Panels A–C show SDS–PAGE gels of the pellets from high-speed cosedimentation

Figure 7. continued

experiments for the tandem CH domain, CH1, and CH2, respectively. Panel D shows the relative fraction of actin bound for the three proteins, calculated from the corrected band intensities from SDS–PAGE (A–C). CH1 binds to F-actin with an affinity similar to that of the full-length tandem CH domain, when compared with that of the CH2 domain.

individual domains, $K_{a,\text{CH1}}$ and $K_{a,\text{CH2}}$. When there is cooperativity, $K_{a,\text{tandem CH}}$ will be multiplied by a factor $K_{\text{CH1–CH2}}$. The $K_{\text{CH1–CH2}}$ value of >1 implies positive cooperativity, and the $K_{\text{CH1–CH2}}$ value of <1 implies negative cooperativity. A $K_{\text{CH1–CH2}}$ equal to 1 implies no cooperativity. Because association constants are the inverse of the dissociation constants in Table 1, $K_{\text{CH1–CH2}} = K_{a,\text{tandem CH}}/(K_{a,\text{CH1}} + K_{a,\text{CH2}}) = (1/K_{d,\text{tandem CH}})/(1/K_{d,\text{CH1}} + 1/K_{d,\text{CH2}}) = 4.7$. This value of $K_{\text{CH1–CH2}}$ corresponds to a $\Delta G_{\text{CH1–CH2}}$ of 0.92 kcal/mol, which is much smaller than the $\Delta G_{a,\text{CH1}}$ of 7.09 kcal/mol corresponding to a $K_{a,\text{CH1}}$ of 1.4×10^5 . This means that the major contribution to the actin binding function of the tandem CH domain is from the intrinsic actin binding affinity of CH1, when compared with the inter-CH domain cooperativity.

DISCUSSION

This study addresses the long-standing question about the role of individual CH domains in the actin binding of tandem CH domains.¹ The quantitative results obtained here confirm qualitative conclusions drawn from previously published studies (discussed in the introductory section).^{18,30} Our results indicate that ABS3 is less important in actin binding than ABS1 and ABS2, because the actin binding function of utrophin is primarily determined by the CH1 domain when compared to the CH2 domain or the cooperativity between the two CH domains.

Why then do the tandem CH domains require CH2 when it is not contributing significantly to actin binding? CH2 might just be offering stability to CH1 against protein aggregation. Starting from the denatured states, CH2 and the full-length tandem CH domain refold completely, whereas all of CH1 aggregates (Figure 2C). Linking CH2 to CH1 is improving the protein stability so that CH1 can bind actin without aggregating. Consistently, most tandem CH domains exist in solution in a closed conformation with significant interactions between the two CH domains,³¹ indicating that the CH1–CH2 interface might be stabilizing the proteins against aggregation. This hypothesis also supports the results from previous cryo-EM studies that suggested that the major role of CH2 might be to impart stability to the tandem domain.³² Additional support for the hypothesis that CH1 is not stable without CH2 comes from the literature: no molecular structures (either X-ray or NMR) are available for the CH1 domains alone, suggesting that they might be quite unstable in the absence of CH2. In contrast, structures have been determined for numerous CH2 domains.³³ In the case of the utrophin tandem CH domain, cryo-EM data have led to the conclusion that it exists in a closed conformation with significant interactions between the two CH domains,²⁹ whereas similar data have been used to conclude that it is in an open conformation with minimal interactions between the two CH domains.^{27,28} Recent studies with site-directed spin labeling and pulsed electron paramagnetic resonance (EPR) show that the utrophin tandem CH domain exists in a dynamic equilibrium between two open

conformations.³⁴ It will be interesting to examine how CH2 stabilizes CH1 in an open conformation, which could provide valuable structural insights into the actin binding function of utrophin tandem CH domain.

How general is this behavior to other tandem CH domains? Because of the aggregation problems associated with truncated proteins, not many data are available in the literature, except in the case of α -actinin.²⁰ The relative order in which the individual CH domains of α -actinin bind to F-actin is consistent with our results for the isolated CH domains of utrophin. The CH1 domain of α -actinin binds to actin much stronger than the corresponding CH2 domain. This similarity between α -actinin and utrophin also validates our folding-upon-binding approach for measuring the actin binding of unstable CH domains. The isolated CH1 and CH2 domains of α -actinin bind to F-actin with K_d values of 57 and >1000 μM , respectively, whereas the full-length tandem CH domain of α -actinin binds to F-actin with a K_d of 4.3 μM .²⁰ These K_d values result in a cooperativity equilibrium constant $K_{\text{CH1-CH2}}$ of 12.5 or a $\Delta G_{\text{CH1-CH2}}$ of 1.51 kcal/mol, which is smaller than the $\Delta G_{\text{a,CH1}}$ of 5.82 kcal/mol corresponding to a $K_{\text{a,CH1}}$ of 1.75×10^4 , implying that the actin binding affinity of α -actinin is primarily determined by its CH1 domain, rather than the inter-CH domain cooperativity or the CH2 domain. To determine whether this behavior is general in terms of the contribution of individual CH domains requires further experiments on tandem CH domains from other proteins. The folding-upon-binding and differential centrifugation techniques developed here will be particularly useful for measuring the actin binding efficiencies of aggregating truncated tandem CH domains.

AUTHOR INFORMATION

Corresponding Author

*Address: 12850 E. Montview Blvd., C238, Skaggs School of Pharmacy and Pharmaceutical Sciences, University of Colorado Anschutz Medical Campus, Aurora, CO 80045. E-mail: krishna.mallela@ucdenver.edu. Phone: (303) 724-3576. Fax: (303) 724-7266.

Author Contributions

[†]S.M.S. and S.B. contributed equally to this work.

Funding

This project was funded by the American Heart Association, a Jane and Charlie Butcher grant in Genomics and Biotechnology, and the ALSAM Foundation through the Skaggs Scholars Program.

Notes

The authors declare no competing financial interest.

ACKNOWLEDGMENTS

We thank Christopher Lima (Sloan-Kettering Institute) for kindly providing the pET-SUMO expression system. We also thank David Bain, Walter Englander, and Deborah Wuttke for many helpful discussions, and David Bain and Walter Englander for their critical reading of the manuscript.

REFERENCES

- Gimona, M., and Winder, S. J. (2008) The calponin homology (CH) domain. In *Protein Science Encyclopedia* (Fersht, A., Ed.) pp 1–16, Wiley-VCH Verlag GmbH & Co. KGaA, Weinheim, Germany.
- Sjöblom, B., Ylänné, J., and Djinović-Carugo, K. (2008) Novel structural insights into F-actin-binding and novel functions of calponin homology domains. *Curr. Opin. Struct. Biol.* 18, 702–708.
- Ervasti, J. M. (2007) Dystrophin, its interactions with other proteins, and implications. *Biochim. Biophys. Acta* 1772, 108–117.
- Singh, S. M., Kongari, N., Cabello-Villegas, J., and Mallela, K. M. G. (2010) Missense mutations in dystrophin that trigger muscular dystrophy decrease protein stability and lead to cross- β aggregates. *Proc. Natl. Acad. Sci. U.S.A.* 107, 15069–15074.
- Henderson, D. M., Lee, A., and Ervasti, J. M. (2010) Disease-causing missense mutations in actin binding domain 1 of dystrophin induce thermodynamic instability and protein aggregation. *Proc. Natl. Acad. Sci. U.S.A.* 107, 9632–9637.
- Blake, D. J., Weir, A., Newey, S. E., and Davies, K. E. (2002) Function and genetics of dystrophin and dystrophin-related proteins in muscle. *Physiol. Rev.* 82, 291–329.
- Miura, P., and Jasmin, B. J. (2006) Utrophin upregulation for treating Duchenne or Becker muscular dystrophy: How close are we? *Trends Mol. Med.* 12, 122–129.
- Odom, G. L., Gregorevic, P., and Chamberlain, J. S. (2007) Viral-mediated gene therapy for the muscular dystrophies: Successes, limitations, and recent advances. *Biochim. Biophys. Acta* 1772, 243–262.
- Sonnemann, K. J., Heun-Johnson, H., Turner, A. J., Baltgalvis, K. A., Lowe, D. A., and Ervasti, J. M. (2009) Functional substitution by TAT-utrophin in dystrophin-deficient mice. *PLoS Med.* 6, e1000083.
- (10) Winder, S. J., Knight, A. E., and Kendrick-Jones, J. (1997) Protein Structure. In *Dystrophin: Gene, protein and cell biology* (Brown, S. C., and Lucy, J. A., Eds.) pp 27–55, Cambridge University Press, Cambridge, U.K.
- Fabbrizio, E., Bonet-Kerrache, A., Leger, J. J., and Mornet, D. (1993) Actin-dystrophin interface. *Biochemistry* 32, 10457–10463.
- Corrado, K., Mills, P. L., and Chamberlain, J. S. (1994) Deletion analysis of the dystrophin-actin binding domain. *FEBS Lett.* 344, 255–260.
- Jarrett, H. W., and Foster, J. L. (1995) Alternate binding of actin and calmodulin to multiple sites on dystrophin. *J. Biol. Chem.* 270, 5578–5586.
- Levine, B. A., Moir, A. J. G., Patchell, V. B., and Perry, S. V. (1990) The interaction of actin with dystrophin. *FEBS Lett.* 263, 159–162.
- Levine, B. A., Moir, A. J. G., Patchell, V. B., and Perry, S. V. (1992) Binding sites involved in the interaction of actin with the N-terminal region of dystrophin. *FEBS Lett.* 298, 44–48.
- Keep, N. H., Winder, S. J., Moores, C. A., Walke, S., Norwood, F. L. M., and Kendrick-Jones, J. (1999) Crystal structure of the actin-binding region of utrophin reveals a head-to-tail dimer. *Structure* 7, 1539–1546.
- Norwood, F. L., Sutherland-Smith, A. J., Keep, N. H., and Kendrick-Jones, J. (2000) The structure of the N-terminal actin-binding domain of human dystrophin and how mutations in this domain may cause Duchenne or Becker muscular dystrophy. *Structure* 8, 481–491.
- Winder, S. J., Hemmings, L., Maciver, S. K., Bolton, S. J., Tinsley, J. M., Davies, K. E., Critchley, D. R., and Kendrick-Jones, J. (1995) Utrophin actin binding domain: Analysis of actin binding and cellular targeting. *J. Cell Sci.* 108, 63–71.
- Morris, G. E., Nguyen, T. M., Nguyen, T. N., Pereboev, A., Kendrick-Jones, J., and Winder, S. J. (1999) Disruption of the utrophin-actin interaction by monoclonal antibodies and prediction of actin-binding surface of utrophin. *Biochem. J.* 337, 119–123.
- Way, M., Pope, B., and Weeds, A. G. (1992) Evidence for functional homology in the F-actin binding domains of gelsolin and α -actinin: Implications for the requirements of severing and capping. *J. Cell Biol.* 119, 835–842.
- Rybakova, I. N., Humston, J. L., Sonnemann, K. J., and Ervasti, J. M. (2006) Dystrophin and utrophin bind actin through distinct modes of contact. *J. Biol. Chem.* 281, 9996–10001.
- Tal, M., Silberstein, A., and Nusser, E. (1985) Why does Coomassie Brilliant Blue R interact differently with different proteins? A partial answer. *J. Biol. Chem.* 260, 9976–9980.

- (23) Mossessova, E., and Lima, C. D. (2000) Ulp1-SUMO crystal structure and genetic analysis reveal conserved interactions and a regulatory element essential for cell growth in yeast. *Mol. Cell* 5, 865–876.
- (24) Gräslund, S., Nordlund, P., Weigelt, J., Hallberg, B. M., Bray, J., Gileadi, O., Knapp, S., Oppermann, U., Arrowsmith, C., Hui, R., Ming, J., dhe-Paganon, S., Park, H.-w., Savchenko, A., Yee, A., Edwards, A., Vincentelli, R., Cambillau, C., Kim, R., Kim, S.-H., Rao, Z., Shi, Y., Terwilliger, T. C., Kim, C.-Y., Hung, L.-W., Waldo, G. S., Peleg, Y., Albeck, S., Unger, T., Dym, O., Prilusky, J., Sussman, J. L., Stevens, R. C., Lesley, S. A., Wilson, I. A., Joachimiak, A., Collart, F., Dementieva, I., Donnelly, M. I., Eschenfeldt, W. H., Kim, Y., Stols, L., Wu, R., Zhou, M., Burley, S. K., Emtage, J. S., Sauder, J. M., Thompson, D., Bain, K., Luz, J., Gheyi, T., Zhang, F., Atwell, S., Almo, S. C., Bonanno, J. B., Fiser, A., Swaminathan, S., Studier, F. W., Chance, M. R., Sali, A., Acton, T. B., Xiao, R., Zhao, L., Ma, L. C., Hunt, J. F., Tong, L., Cunningham, K., Inouye, M., Anderson, S., Janjua, H., Shastry, R., Ho, C. K., Wang, D., Wang, H., Jiang, M., Montelione, G. T., Stuart, D. I., Owens, R. J., Daenke, S., Schütz, A., Heinemann, U., Yokoyama, S., Büssow, K., and Gunsalus, K. C. (2008) Protein production and purification. *Nat. Methods* 5, 135–146.
- (25) Carson, M., Johnson, D. H., McDonald, H., Brouillette, C., and DeLucas, L. J. (2007) His-tag impact on structure. *Acta Crystallogr. D63*, 295–301.
- (26) Keep, N. H., Norwood, F. L. M., Moores, C. A., Winder, S. J., and Kendrick-Jones, J. (1999) The 2.0 Å structure of the second calponin homology domain from the actin-binding region of the dystrophin homologue utrophin. *J. Mol. Biol.* 285, 1257–1264.
- (27) Moores, C. A., Keep, N. H., and Kendrick-Jones, J. (2000) Structure of the utrophin actin-binding domain bound to F-actin reveals binding by an induced fit mechanism. *J. Mol. Biol.* 297, 465–480.
- (28) Galkin, V. E., Orlova, A., VanLoock, M. S., Rybakova, I. N., Ervasti, J. M., and Egelman, E. H. (2002) The utrophin actin-binding domain binds F-actin in two different modes: Implications for the spectrin superfamily of proteins. *J. Cell Biol.* 157, 243–251.
- (29) Sutherland-Smith, A. J., Moores, C. A., Norwood, F. L. M., Hatch, V., Craig, R., Kendrick-Jones, J., and Lehman, W. (2003) An atomic model for actin binding by the CH domains and spectrin-repeat modules of utrophin and dystrophin. *J. Mol. Biol.* 329, 15–33.
- (30) Gimona, M., and Winder, S. J. (1998) Single calponin homology domains are not actin-binding domains. *Curr. Biol.* 8, R674–R675.
- (31) Singh, S. M., and Mallela, K. M. G. (2012) The N-terminal actin-binding tandem calponin-homology (CH) domain of dystrophin is in a closed conformation in solution and when bound to F-actin. *Biophys. J.* 103, 1970–1978.
- (32) McGough, A., Way, M., and DeRosier, D. (1994) Determination of the α -actinin-binding site on actin filaments by cryoelectron microscopy and image analysis. *J. Cell Biol.* 126, 433–443.
- (33) Gimona, M., and Winder, S. J. (2005) The calponin homology (CH) domain. In *Modular protein domains* (Cesareni, G., Gimona, M., Sudol, M., and Yaffe, M., Eds.) Wiley-VCH Verlag GmbH & Co. KGaA, Weinheim, Germany.
- (34) Lin, A. Y., Prochniewicz, E., James, Z. M., Svensson, B., and Thomas, D. D. (2011) Large-scale opening of utrophin's tandem calponin homology (CH) domains upon actin binding by an induced-fit mechanism. *Proc. Natl. Acad. Sci. U.S.A.* 108, 12729–12733.
- (35) Singh, S. M., Molas, J. F., Kongari, N., Bandi, S., Armstrong, G. S., Winder, S. J., and Mallela, K. M. G. (2012) Thermodynamic stability, unfolding kinetics, and aggregation of the N-terminal actin binding domains of utrophin and dystrophin. *Proteins: Struct., Funct., Bioinf.* 80, 1377–1392.